

Physico-chemical parameters governing protein microencapsulation into biodegradable polyesters by coacervation

Claudio Thomasin, Hans P. Merkle, Bruno A. Gander *

Department of Pharmacy, ETH, Winterthurerstr. 180, 8057 Zürich, Switzerland

Received 10 June 1996; received in revised form 14 October 1996; accepted 13 November 1996

Abstract

Coacervation of various PLAs (poly(D,L-lactic acid)) and PLGAs (poly(D,L-lactic-co-glycolic acid)) was studied for microencapsulation of BSA powder and aqueous BSA solution, focusing on the interfacial properties between coacervate, continuous liquid and solid or aqueous BSA and on selected process parameters. From interfacial tensions and contact angles, the necessary conditions for successful entrapment of both solid and aqueous BSA were given in a coacervation system using either dichloromethane or ethyl acetate as polymer solvents and silicone oil as the coacervating agent. Spreading coefficients were positive at the coacervate/aqueous BSA interface ($0.2\text{--}2.6\text{ mN m}^{-1}$), but negative between continuous liquid and aqueous BSA. For solid BSA, work of adhesion to the coacervate was substantially higher ($41\text{--}52\text{ mN m}^{-1}$) than to the continuous liquid ($20\text{--}35\text{ mN m}^{-1}$). The process parameters, physical state and particle size of the protein, amount and viscosity of the coacervating agent, type and \bar{M}_w of polymer, nominal protein loading and amount of aqueous protein solution were the most critical with respect to encapsulation efficiency and burst release. Highest encapsulation efficiency (60–80%) and acceptable burst release (< 20%) were found with micronized and aqueous BSA at low (1%) nominal loading, using a hydrophilic low \bar{M}_w polymer and a coacervating agent of moderate viscosity (100–1000 mPa s). © 1997 Elsevier Science B.V.

Keywords: Biodegradable microspheres; PLA; PLGA; Coacervation; Interfacial properties; Protein delivery

1. Introduction

The design of new and improvement of existing controlled release delivery systems for peptide and protein drug has become an important focus both in academia and industry. Among the first recog-

* Corresponding author. Tel.: +41 1 2576012; fax: +41 1 2625459; e-mail: bruno.gander@pharma.ethz.ch

nising the potential of microencapsulated peptides and proteins was Chang (1976), who reported on the feasibility of microencapsulated drugs, especially hormones, enzymes and vaccines for long-term treatment of diseases. Later, a phase separation method was described to entrap nafarelin, a LH-RH analogue, into biodegradable lactide/glycolide polymers (Sanders et al., 1984, 1985). Moreover, several patent applications were filed for polyester coacervation processes (Orsolini et al., 1986; Lapka et al., 1986; Sandow and Seidel, 1986; Lewis and Sherman, 1989; Komen and Groennendaal, 1991; Lawter and Lanzilotti, 1992; Nerlich et al., 1993). However, still limited information is available describing the mechanism and critical parameters of polyester coacervation and the consequence for drug entrapment and the quality of microspheres. The delicate balance and interactions between the active compound, the polymer and the manufacturing variables were pointed out by Kissel and Demirdere (1987) for the microencapsulation of bromocriptin. More specifically, physico-chemical characteristics of PLGA were considered for the microencapsulation of peptides by coacervation (Ruiz et al., 1989, 1990; Nihant et al., 1995). Recently, an improved coacervation method has been proposed to prepare small-sized (1–10 μm) ovalbumin loaded microspheres for oral administration (McGee et al., 1994). The main objectives of this study were to determine the behaviour of the model protein BSA at the coacervate/continuous liquid interface and to define the relevance for protein entrapment. Moreover, key-parameters of polyester coacervation should be revealed and related to microsphere morphology, protein encapsulation and initial release behaviour.

2. Theoretical background

The interfacial tensions between the active compound and the coacervate/continuous phases (Fig. 1) are considered essential driving forces for drug microencapsulation (Green, 1979).

For an aqueous protein solution, successful entrapment in a coacervate phase depends on the respective spreading coefficients (S):

$$S_{P1/P3} = \gamma_{P2/P3} - (\gamma_{P1/P2} + \gamma_{P1/P3}) \quad (1)$$

$$S_{P2/P3} = \gamma_{P1/P3} - (\gamma_{P1/P2} + \gamma_{P2/P3}) \quad (2)$$

Consequently, encapsulation can be expected if:

$$S_{P1/P3} < S_{P2/P3} \quad (3)$$

For solid BSA particles, entrapment depends on the spreading behaviour of the liquid coacervate phase on the particles' surface. Wetting is favoured by a high surface free energy of the solid, as expressed by γ_{sv} , a low surface free energy of the liquid (γ_{lv}), and by a low solid/liquid interfacial free energy (γ_{sl}), as defined by the equation of Young (1855):

$$\gamma_{sv} = \gamma_{sl} + \gamma_{lv} \cos \theta \quad (4)$$

Combining with Dupre's concept of work of adhesion (Dupre, 1869), the Young-Dupre equation is obtained (Eq. (5)), which relates the work of adhesion (W_a) between solid material and wetting liquid to the contact angle (θ) and the surface tension of the liquid (γ_{lv}).

$$W_a = \gamma_{lv}(1 + \cos \theta) \quad (5)$$

It should be considered, however, that the wetting behaviour of a liquid phase in contact with a vapour environment does not represent the conditions met in the coacervation mixture itself. This difference can be accounted for by calculating the spreading coefficient S in the coacervation dispersion (Eq. (2)), and hence, the drug entrapment by the coacervate phase becomes predictable. If the solid surface tension (γ_{sv}) is known, γ_{sl} for the interfaces coacervate/solid core ($\gamma_{P2/P3}$) and con-

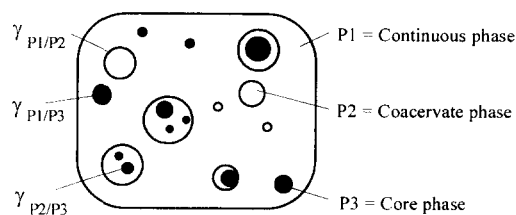


Fig. 1. Coacervation mixture with aqueous protein microdroplets (P3) to be encapsulated by the coacervate phase (P2); empty and protein-loaded coacervate droplets are immersed in the continuous liquid (P1). $\gamma_{(P1/P3)}$, $\gamma_{(P2/P3)}$ and $\gamma_{(P1/P2)}$ represent the interfacial tensions between the different phases.

tinuous liquid/solid core ($\gamma_{P1/P3}$) may be determined according to Young's law (Eq. (4)).

3. Materials and methods

3.1. Material

Poly(D,L-lactic acid) [PLA] (Resomer[®] R 202 and R 206), poly(L-lactic acid) [PLLA] (Resomer[®] L 206), poly(D,L-lactic-co-glycolic acid) 75:25 [PLGA 75:25] (Resomer[®] RG 752 and RG 755), and poly(D,L-lactic-co-glycolic acid) 50:50 [PLGA 50:50] (Resomer[®] RG 502) were purchased from Boehringer Ingelheim, D-Ingelheim. Dichloromethane [DCM] and ethyl acetate [EtAc], both of analytical grade (>99.5%), were from Merck, D-Darmstadt, hexane [Hex] and silicone oil DC-200 [PDMS] of different viscosities (110, 375, 1070 mPa s) were from Fluka, CH-Buchs, and octamethylcyclotetrasiloxane [OMCTS] from Scheller, CH-Zurich. PDMS of 3000 mPa s was prepared by mixing individual amounts of PDMS 1070 mPa s and PDMS 10 700 mPa s (Plüss and Stauffer, CH-Oftringen) according to a viscosity nomogram from Dow Corning, Midland, USA. All other compounds were of analytical grade, or as stated below.

3.2. Interfacial tension and contact angle between the components of coacervation mixtures

Coacervate phase and continuous liquid were obtained by dissolving PLA R 202 in DCM or EtAc at a concentration of 5% (w/w) and inducing phase separation through PDMS addition. The coacervation mixture was transferred into screw-capped tubes and centrifuged at 4000 rev min⁻¹ to separate both phases. Completeness of separation was examined microscopically. The density of the continuous and coacervate phases was measured with a densitometer (Paar 46, A-Gratz). The interfacial tension between aqueous BSA (5%) and coacervate phase, and between continuous liquid and coacervate phase was determined by spinning drop tensiometry (SITE 03, Krüss, D-Hamburg). For this, the rotating tube was filled with the coacervate, followed by

injection of 1–3 μ l of either aqueous BSA or continuous liquid by means of a syringe. The dimension of the drop was measured at increasing rotational rate of 2000–9000 rev min⁻¹. Provided the ratio of drop length over diameter was at least 4:1, the interfacial tension was calculated according to:

$$\gamma = e(vd)^3 n^2 \Delta\rho \quad (6)$$

Here, γ (mN m⁻¹) is the interfacial tension, e (mN cm³ min² m⁻¹ g⁻¹ mm⁻³) the apparatus constant, v (mm s dv⁻¹) the magnification factor, d (sdv) the drop diameter, n (min⁻¹) the rotational speed of the filled tube, and $\Delta\rho$ (g cm⁻³) is the density difference between the two phases.

Surface tensions of the various liquids and the interfacial tension between aqueous BSA and continuous liquid was also measured at 20°C by a ring tensiometer (K10, Krüss, D-Hamburg), without correcting for the density difference of the two phases (Zuidema and Waters, 1941).

Wetting and spreading behaviour of coacervate and continuous liquid drops on compacted (550 MPa, 15 mm in diameter) BSA disks was determined by contact angle measurement using the sessile drop technique (Anglometer, DW2, Krüss, D-Hamburg). The polar and dispersive contribution to the surface tension of BSA was calculated according to the method of Owens and Wendt (1969) with water and diiodomethane.

3.3. Milling of BSA powder

Previous to microencapsulation of BSA powder, the native lyophilised product with a particle size of 0.5 to 2 mm was ground in a ball mill (Fritsch Pulverisette, Fritsch, D-Idar-Oberstein), rotated at 350 min⁻¹ for 30 min. The milled powder was dispersed in hexane, wet-sieved through mesh sizes of 50, 20 and 10 μ m by ultrasonication (A 75 NS, Alpine D-Augsburg) and dried at reduced pressure. Micronized powder was obtained by processing ball-milled BSA in a counterjet air-mill (GEM-T, Helme products, New Jersey, USA) at a pressure of 6 bar.

3.4. Microencapsulation of the model protein BSA

Solid and aqueous BSA were microencapsulated by a phase separation process as described by Fong (1979), Sanders et al. (1984) and Ruiz et al. (1989). Typically, 2 g of polymer were dissolved in DCM or EtAc at initial concentrations ranging from 2.5 to 10% (w/w). Half of this solution was transferred into a jacketed reaction vessel with a four-necked lid (250 ml, Schmizo PS 98, CH-Zofingen) and equipped with three baffles and an anchor-shaped glass stirrer. Either 20–200 mg of solid protein powder or 500–1500 μ l of aqueous BSA solution were finely dispersed in the remaining cooled (0–5°C) polymer solution by ultrasonication at output 7 for 60 s (Vibra cell VC 375, Sonics and Materials, Danbury, USA), and transferred into the vessel. Under stirring at 1000 rev min⁻¹ (IKA, RE 162, Janke and Kunkel, D-Staufen) and at a temperature of 10–15°C, coacervation was induced by introducing a predetermined amount of silicone oil at a rate of 4 g min⁻¹ (peristaltic pump MP4, Ismatec, CH-Zurich). After completion of silicone oil addition, stirring was continued for 15 min. Hardening of the coacervate droplets was performed by transferring the coacervation mixture through a PTFE-tube into a second vessel (Schmizo PS 137, CH-Zofingen), equipped with a cage-stirrer and containing 1200 ml of hardening agent. Stirring was continued at 350 rev min⁻¹ for 60 min (IKA, RE 16, Janke and Kunkel, D-Staufen). Microspheres were collected on a sintered glass filter and washed several times with a total of 100 ml of hexane to remove PDMS. The microparticles were air-dried for 5 min and resuspended three times in 100 ml of aqueous 0.1% Synperonic F 68 (ICI, Cleveland UK). After washing, the powder was dried for 12 h in a drying chamber (RT, 100 mbar) over phosphor(V)-oxide (Sicapent[®], Merck, D-Darmstadt).

3.5. Morphology and particle size distribution of the microspheres

For morphological examination, the micro-

spheres were mounted on double-faced adhesive tape, sputtered with platinum and viewed in a Hitachi S-700 scanning electron microscope. Protein loaded microspheres were also examined by light microscopy and microphotographed (Nikon Optiphot, Nikon, JPN-Tokyo).

The microsphere sizes were measured by laser light scattering (Mastersizer X, Malvern, UK) and analysed using Mie's theory, accounting for the optical properties of the polymer used. The refractive index of PLA and PLGA was determined according to a group contribution method, suggested by Van Krevelen (1990).

3.6. Encapsulation efficiency

Protein content was determined with 20–30 mg of BSA-loaded microspheres dissolved in 2 ml of DCM; the dispersion was vacuum-filtered on a microporous membrane (regenerated cellulose RC58, 0.20 μ m, Schleicher and Schüll, D-Dassel). Filters were washed three times with DCM and air-dried. After drying, BSA was eluted three times with 3 ml phosphate buffered saline pH 7.4, containing 0.02% sodium azide as preservative. The solution was analysed either by a colorimetric protein assay (Bradford, 1976) based on coomassie-brilliant blue (Bio Rad, D-Munich) or fluorometrically (Fluoromax, Spex Industries, NJ-Edison) with excitation and emission wavelengths of 278 and 340 nm, respectively.

3.7. Burst release

The initial release of protein from microspheres was determined in screw cap borosilicate vials (Chromacol, London, UK) with 50 mg of microspheres dispersed in 4.0 ml of phosphate buffered saline pH 7.4 and preserved with 0.02% sodium azide. The dispersion was ultrasonicated to facilitate wetting and the vials fixed horizontally in a drum rotating at 3 rev min⁻¹ at 37°C. After 24 h, the dispersion was centrifuged and the supernatant assayed fluorometrically.

Table 1

Characteristics of different interfaces present in the coacervation mixtures with aqueous BSA (5%, w/w) used as core material (values are represented as mean \pm S.D., $n = 3$)

Composition of coacervation mixture (%)				Interfacial tension ^a , γ , and spreading coefficient, S (mN m ⁻¹)				
PLA	DCM	EtAc	PDMS	Continuous liquid/BSA (P1/P3)		Coacervate/BSA (P2/P3)		Continuous liquid/coacervate (P1/P2)
				γ	S	γ	S	γ
3.0	58.0	—	39.0	7.5 \pm 0.2	-3.0	5.4 \pm 0.2	1.2	0.9 \pm 0.0
2.5	48.5	—	49.0	10.1 \pm 0.5	-5.4	6.2 \pm 0.4	2.4	1.5 \pm 0.0
3.0	—	58.0	39.0	5.2 \pm 0.1	-1.4	4.4 \pm 0.2	0.2	0.6 \pm 0.1
2.5	—	48.5	49.0	6.3 \pm 0.1	-4.2	2.9 \pm 0.3	2.6	0.8 \pm 0.1

^a The *n*-octanol/water interface was used as reference ($\gamma = 8.5$ mN m⁻¹, 20°C; Weast et al., 1989); experimentally determined values were 8.5 \pm 0.6 and 8.3 \pm 0.3 mN m⁻¹ for spinning drop and ring tensiometry, respectively.

4. Results

4.1. Interfacial properties of the different phases present in the coacervation mixtures

According to established phase diagrams (Thomasin et al., 1996b), PLA/DCM/PDMS and PLA/EtAc/PDMS mixtures at two different ratios of solvent/coacervating agent were analysed to examine the effect of solvent type and coacervation composition on the interfacial tension. With the mixtures, an early coacervation stage with still unstable droplets was mimicked, where wetting and spreading are most probably crucial for the engulfment of core material. From the values of Table 1, the interfacial tensions between core material and continuous phase ($\gamma_{P1/P3}$) were significantly higher (Student's *t*-test) than those ($\gamma_{P2/P3}$) of coacervate/BSA. The lowest free energy was found for the interface between continuous liquid and coacervate ($\gamma_{P1/P2}$). Consequently, the calculated spreading coefficients between continuous liquid and BSA-solution ($S_{P1/P3}$) were negative, whereas they were positive for the coacervate/BSA interface. According to Eq. (3), the coacervate phase spread therefore spontaneously on the aqueous BSA-surface, whereas the continuous phase did not. Hence, the conditions for successful encapsulation into PLA coacervate droplets were fulfilled. Incidentally, all γ -values were lower for the EtAc/PDMS mixture as compared to

DCM/PDMS.

Interfacial characteristics relevant for the engulfment of solid BSA are given in Table 2.

The surface tension values of the continuous liquid (P1) and of the corresponding coacervate phase (P2) were comparable for both solvent systems. For the DCM system, the contact angle between continuous liquid and BSA was substantially lower than that between coacervate and BSA. Conversely, for the EtAc system, the θ values were quite similar. Although good wetting of BSA was indicated by the low contact angles, the liquid phases did not spread spontaneously (i.e. $\theta = 0$) on solid BSA. In terms of work of adhesion, W_a values indicated stronger interaction between solid BSA and coacervate than between BSA and continuous liquid.

Calculation of the spreading coefficient, S , between, respectively, the coacervate or continuous phases and solid BSA requires the knowledge of the surface tension of solid BSA (γ_{sv}) (Eq. (2)). For γ_{sv} , a value of 48 mN m⁻¹ with dispersive and polar contributions of 37 mN m⁻¹ and 11 mN m⁻¹, respectively, was found for BSA, as determined by the Owens-Wendt method using water and diiodomethane. On the basis of these data, the calculated interfacial tensions (Eq. (4)) of coacervate/solid BSA ($\gamma_{P2/P3}$) and continuous phase/solid BSA ($\gamma_{P1/P3}$) were 22.7 and 26.0 mN m⁻¹, respectively, for the DCM system, and 29.3 and 30.0 mN m⁻¹, respectively, for the EtAc

Table 2

Surface tension, γ_{lv} , of the continuous liquid (P1) and coacervate (P2), contact angle, Θ , work of adhesion, W_a , and spreading coefficient, S , between, respectively, the continuous (P1) or coacervate (P2) phases and solid BSA

Polymer solvent	γ_{lv} (mN m ⁻¹)		θ (°)		W_a (mN m ⁻¹) ^a		S (mN m ⁻¹) ^b	
	P1	P2	P1/P3	P2/P3	P1/P3	P2/P3	P1/P3	P2/P3
DCM	24.0	26.9	24	45.9	20	52.2	-3.9	2.7
EtAc	21.3	22.8	33	39.2	35	41.5	-1.3	0.1

The composition of the coacervation mixtures used was 3% PLA, 58% DCM or EtAc, and 39% PDMS.

^a Calculated according Eq. (5).

^b Calculated according Eqs. (2) and (4).

system. Thus, spreading of DCM and EtAc coacervate on solid BSA was spontaneous ($S = 2.7$ and 0.1 mN m⁻¹, respectively). By contrast, negative spreading coefficients resulted for the interface continuous liquid/solid BSA in both the DCM and EtAc systems (Eq. (1)). Wetting of a solid core by a coacervate requires a core/coacervate affinity dominating over that of core/continuous liquid. As shown by the spreading coefficients, this requirement was fulfilled for both solvent systems.

4.2. Microencapsulation of solid BSA

4.2.1. Morphology and size distribution of the microspheres

Optical transmission and scanning electron micrographs of PLA and PLGA microspheres loaded with BSA powder revealed regular shape and particle sizes in the range of 20–100 μ m (Figs. 2 and 3). Fig. 2 shows that micronized BSA particles were quite regularly dispersed in the PLA matrix, with most of the protein particles being in an agglomerated state and oriented more towards the centre rather than to the periphery of the microspheres. Fig. 3 shows PLGA microspheres with a smooth surface morphology and without any visible pinholes, cracks or pores. This type of morphology was found for all polyester types when solid BSA was microencapsulated.

Typical particle size distributions showed undersize diameters $D(v,10)$ of 11–16 μ m, $D(v,50)$ of 22–35 μ m and $D(v,90)$ of 33–68 μ m. Both the nominal BSA loading (1, 3, 5 and 10%) and the BSA particle size (< 10, 10–20 and 20–50 μ m)

only affected marginally the values of $D(v,10)$ and $D(v,50)$. $D(v,90)$, however, increased significantly (34, 35, 42 and 68 μ m) with increasing nominal BSA loading. Therefore, a considerable volume fraction of microspheres was smaller in size than the BSA particles used. Consequently, many microspheres must have remained unloaded contributing possibly to lower encapsulation efficiency.

4.2.2. Encapsulation efficiency and burst release

For microencapsulation of BSA powder, the effect of three parameters on the encapsulation efficiency and burst release, observed after 24 h, were studied: (i) BSA particle size, (ii) BSA nominal loading, and (iii) polymer type and molecular weight. The entrapment efficiency was inversely related to the particle size of the core material (Fig. 4). Loading efficiency was increased from 57

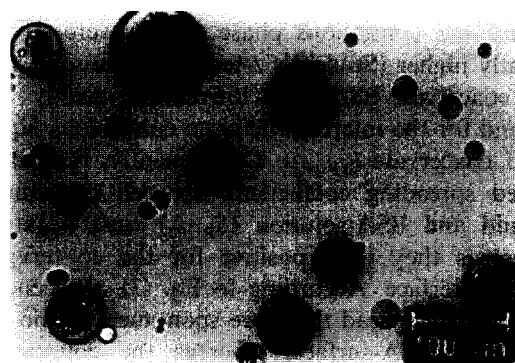


Fig. 2. Optical transmission micrograph of poly(*l*-lactide) microspheres loaded with 10% micronized BSA. Agglomerated core material is embedded in the polymer matrix. The bar represents 100 μ m.

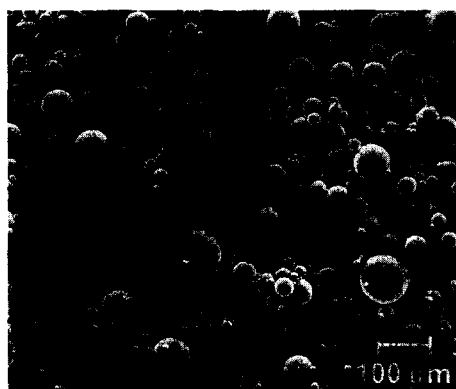


Fig. 3. SEM-micrograph of 68.8 kDa PLGA 75:25 microspheres loaded with nominal 1% micronized BSA of high molecular weight. The bar represents 100 μm .

to 90% if micronized powder was encapsulated. Concomitantly, the burst release decreased from 90 to 23% of the actual dose (Fig. 4A). Increasing nominal amounts (1–10%, w/w) of micronized BSA had a marked effect on the burst release but not on the efficiency (Fig. 4B). At low BSA content (1–3%), the burst release increased only slightly from 23 to 31%. Microspheres with a higher protein content, however, released nearly all of the encapsulated material within 1 day.

Finally, polymer type and polymer molecular weight were of minor importance for the loading efficiency, which was in the order of 79%, but exerted an important effect on the burst release. Typically, low \bar{M}_w (17.2 kDa) PLGA 75:25 microspheres showed a burst release of approximately 21% as compared to only 10% with the high molecular weight ($\bar{M}_w = 68\,600$) PLGA 75:25 preparations. Similarly, the semicrystalline PLLA ($\bar{M}_w = 69.5$ kDa) yielded BSA loading efficiencies of 86 and 75% at nominal loadings of 1 and 10 $\mu\text{g mg}^{-1}$ microspheres, respectively. The burst release was less than 10% and seemed to be independent of the nominal loading.

4.3. Microencapsulation of aqueous BSA solutions

The investigated parameters susceptible to affect the microencapsulation of an aqueous protein solution are compiled in Table 3.

4.3.1. Morphology, particle size distribution and yield

Optical transmission micrographs of PLA coacervate droplets loaded with aqueous BSA droplets revealed a multicore matrix structure with the aqueous microdroplets being dispersed relatively homogeneously within the coacervate phase (Fig. 5). This structure of the coacervate phase may well provide a realistic picture of the internal morphology of the final microspheres. In contrast to the microspheres loaded with solid BSA, those containing aqueous BSA did not reveal their internal morphology by light microscopy. However, the surface morphology of the microspheres loaded with aqueous BSA was slightly porous. Qualitatively, porosity seemed to depend highly on the amount of aqueous phase used for microencapsulation and on the drying conditions, as detailed elsewhere (Thomasin et al., 1996b). Clearly, encapsulation of increasing aqueous phase volumes exerted a plasticizing effect on the polymer matrix, rendering the drying conditions more critical. When drying was performed at relatively low air pressure (0.5 or 5 mbar), the microspheres loaded with volumes of protein solution as large as 1000 or 1500 μl per 2 g polymer showed massive pores and cracks.

Only particles less than 180 μm were characterised here, as only such small microspheres are of practical interest for parenteral administration by syringes. The yield of microspheres, as collected after drying, was generally 80–90%. Yields were slightly lower (70–75%) if the concentration of the polymer solution for coacervation was 2.5% rather than 5 or 10% (Table 3). In contrast, the low viscous coacervating agent PDMS 110 mPa s gave a yield of only 47%, which was due to the substantial amount of aggregates. The viscosity of the coacervating agent also greatly affected the microsphere size distribution. Thanks to the stabilising effect of highly viscous coacervating agent, narrow size ranges of 8–33 and 8–40 μm were achieved with PDMS 3000 and 1070 mPa s, respectively. Substantially larger particle sizes were obtained when PDMS 375 mPa s (80% within 15–47 μm) or PDMS 110 mPa s (47% within 36–171 μm) were used. Besides the non-solvent viscosity, polymer concentration and \bar{M}_w

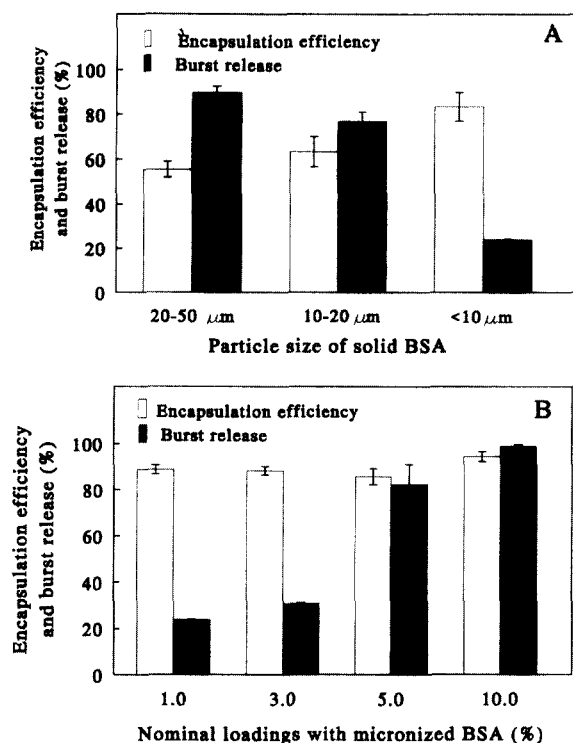


Fig. 4. Encapsulation efficiency and burst release after 24 h for PLGA 75:25 microspheres: effect of BSA particle size (A) and of nominal BSA loading (B).

also influenced particle sizes with the smallest microspheres (5–22 μm) being produced when PLA of 14.6 kDa at low polymer concentration (2.5%) was coacervated by the highly viscous PDMS 1070 mPa s. Prepared under identical conditions, 130 kDa PLA yielded particle sizes of 24–85 μm . Moreover, the type of polymer solvent and the solvent/non-solvent ratio also affected the particle sizes. For a given solvent/PDMS weight ratio (e.g. 1:2.75), EtAc produced larger particles (14–80 μm) than DCM (8–33 μm), indicating increased coalescence of coacervate droplets due to weakened EtAc-PDMS interaction (Thomasin et al., 1996c). Finally, the mean particle size was reduced from 45 to 22 μm , when the solvent/non-solvent ratio was increased from 1:1.5 to 1:2.75. Higher PDMS concentration resulted in increased continuous phase viscosity, which promoted efficiently the break-up of coacervate droplets and prevented coalescence.

4.3.2. Encapsulation efficiency and burst release

Variation of the solvent type and solvent/coacervating agent ratio showed that BSA entrapment was less effective in the EtAc-PLA than in the DCM-PLA system. Also, increasing amounts of PDMS in EtAc-PLA stabilised the coacervate droplets against merging and improved BSA entrapment. Concomitantly, the fraction released after 24 h decreased from 79 to 12%. Microspheres prepared in DCM/PDMS showed significantly higher loading efficiencies (57–64%). However, a trend comparable to the EtAc-system was observed for the burst release. The amount of active compound released was lowered from 51.6 to 5.3% with increasing proportions of PDMS.

Variation of the the coacervating agent viscosity within the range of 110 to 1070 mPa s did not markedly influence the BSA entrapment efficiency (62–64%). Only the batch prepared with the 3000 mPa s PDMS showed a significantly lower entrapment efficiency. The burst release, on the other hand, did not differ greatly between the two preparations made with PDMS 375 and 1070 mPa s. Incidentally, this demonstrates that the very slight difference in particle sizes of the latter two products, i.e. 15–47 and 8–40 μm , was not critical for the initial release. By contrast, the microspheres prepared with the 110 mPa s PDMS showed a very low (4%) and those made with the 3000 mPa s PDMS a very high (42%) burst release. We may assume that the larger size (36–71 μm) of the microspheres prepared with the 110 mPa s PDMS is partly responsible for the lower burst release.

For studying the importance of polymer \bar{M}_w and initial concentration, the volume ratio of BSA/polymer solutions and the amount of added PDMS were kept constant, although this resulted in suboptimal coacervation conditions. It appeared that satisfactory encapsulation efficiency (63%) could be obtained only with the 10% PLA-14.6 kDa, whereas quite low entrapment efficiencies (24–30%) were found for the 130 kDa PLA and for the lower concentrations of the 14.6 kDa PLA. Interestingly, however, the 130 kDa PLA

Table 3

Influence of process parameters on the characteristics of 14.6 kDa PLA microspheres loaded with aqueous BSA

Process parameters		Yield of microspheres < 180 μ m (%)	Encapsulation efficiency (%)	Burst release after 24 h (%)
Type of solvent and weight ratio solvent/coacervating agent				
EtAc/PDMS	1:1.50	—	Very unstable coacervates	
	1:2.75	85.3	23.0 \pm 0.90	79.2 \pm 3.81
	1:4.00	84.5 \pm 2.7 ^a	45.2 \pm 4.73	12.2 \pm 3.89
DCM/PDMS	1:1.50	85.4	64.3 \pm 1.12	51.6 \pm 3.42
	1:2.75	86.0 \pm 3.3 ^a	63.6 \pm 5.40	14.2 \pm 5.27
	1:4.00	84.9	56.9 \pm 3.12	5.3 \pm 1.08
Viscosity of the coacervating agent, PDMS (mPa s)				
	110	46.6	62.8 \pm 4.10	3.7 \pm 0.60
	375	83.6 \pm 1.3 ^a	61.7 \pm 7.37	19.2 \pm 3.58
	1070	86.0 \pm 3.3 ^a	63.6 \pm 5.40	14.2 \pm 5.27
	3000	86.7	45.0 \pm 6.20	41.7 \pm 5.65
Polymer molecular weight and initial polymer concentration (%)				
PLA (14.6 kDa)	2.5	70.9	28.7 \pm 1.42	51.0 \pm 0.63
	5.0	83.0	30.0 \pm 2.50	46.5 \pm 0.93
	10.0	86.0 \pm 3.3 ^a	63.6 \pm 5.40	14.2 \pm 5.27
PLA (130 kDa)	2.5 ^b	75.0	24.2 \pm 3.77	5.1 \pm 0.72
	5.0 ^b	87.8	26.7 \pm 5.42	5.8 \pm 0.46
	10.0 ^b	Too viscous to handle		
Volume of protein solution, V (μl), and nominal loading level, D (%)				
V: 500	D: 1.0	86.0 \pm 3.3 ^a	63.4 \pm 1.68	14.2 \pm 5.27
1000	D: 2.5	89.8	63.6 \pm 5.40	44.5 \pm 1.82
1500	D: 4.0	84.2	69.6 \pm 2.04	49.0 \pm 1.92

Unless specified otherwise, nominal BSA loading was 1% (w/w), the initial PLA concentration 10% (w/w), the volume of BSA solution 500 μ l, and the viscosity of the PDMS used 1070 mPa s.

^a The values represent mean \pm S.D. of three individual batches.

^b Nominal loading was 2%.

showed very low burst release. Burst release was also acceptable for the 14.6 kDa PLA used at a concentration of 10%, but was too high when this polymer was used at lower concentrations.

The volume of water necessary to dissolve a specific amount of protein may differ from one compound to another. When the volume of protein solution was raised from 500 to 1500 μ l per 2 g polymer, the encapsulation efficiency was not significantly changed, although the lower volume of protein droplets was assumed to lead to an improved uptake into the coacervate phase. On the other hand, burst release increased very markedly (from 14 to 49%) with increasing nominal loading and volume of aqueous phase. This may be explained, at least partly, by the more

pronounced surface porosity of these preparations as observed on the SEM micrographs (data not shown). This again suggests that microparticles prepared with a larger proportion of aqueous phase risk to become porous when dried under the relatively stringent conditions of 5 mbar.

4.4. Microspheres loaded with solid versus aqueous BSA

Fig. 6 compares the extent of burst release between the microspheres loaded with either solid or aqueous BSA. For all polymers tested, micronized BSA yielded a much higher burst than BSA entrapped as aqueous solution. This suggests that relatively large solid BSA particles were prob-

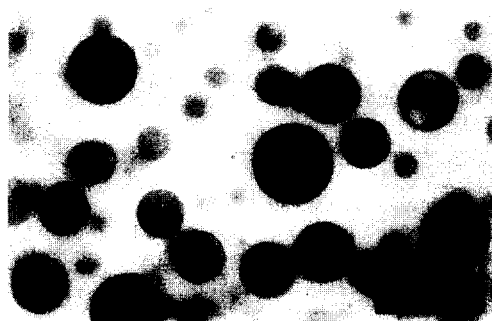


Fig. 5. Optical transmission micrograph of PLA coacervate droplets loaded with aqueous BSA droplets. The bar represents 50 μm .

ably coated with a thinner polymer layer than the much smaller protein droplets, which had an average size of a few micrometers. Interestingly, PLGA 75:25 engulfed the aqueous protein more readily than the more hydrophobic PLA, which is reflected by the significantly higher loading and lower burst release. Finally, PLA released more protein within 24 h than the more hydrophilic copolymers. This may be explained by the observed faster swelling of the more hydrophilic PLGA microspheres, leading to substantial particle aggregation over the first few hours and, hence, to a reduced total surface area for protein release.

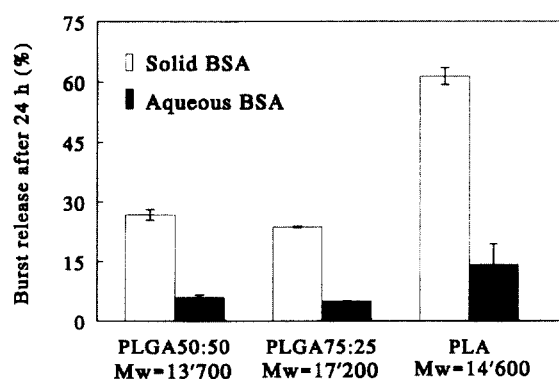


Fig. 6. Effect of the solid versus liquid state of core material on the burst release of BSA from microspheres of PLA and PLGA. The actual loadings (in %, w/w) were 0.81, 0.86 and 0.69 for the solid BSA in PLGA 50:50, PLGA 75:25 and PLA, respectively, and 0.78, 0.73 and 0.63 for the aqueous BSA in PLGA 50:50, PLGA 75:25 and PLA, respectively.

5. Discussion

Coacervation is generally considered suitable for microencapsulation of water-soluble compounds, as satisfactory loading levels and efficiencies can be achieved (Fong, 1988). The present study revealed essential physico-chemical properties of the core material and of the coacervation mixture.

5.1. Interfacial properties

An important prerequisite for studying interfacial properties in coacervation mixtures containing solid or dissolved protein is sufficient stability of the protein compound. BSA has indeed been reported to be stable in contact with organic solvents (Hora et al., 1990; Cohen et al., 1991), in contrast to other proteins for which aggregation and denaturation at W/O interfaces has been reported (Cohen et al., 1991; Lu and Park, 1995). On the other hand, coacervate phases themselves require also some degree of stability for interfacial characterisation. For this reason, PLA was preferred to PLGA 50:50, which has been shown recently to gel and precipitate upon desolvation or in contact with aqueous protein solution (Nihant et al., 1995), rendering interfacial measurements difficult. However, data obtained from interfacial measurements using separated phases reflect only partly the properties within the coacervation mixture. As an example, the surface tension of fully hydrated human serum albumin decreased from 70 mN m^{-1} in phosphate buffer to 50 mN m^{-1} when deposited on a polymer surface (Absolom et al., 1987). Interfacial properties were also considered for insulin ($\gamma_{\text{sv}} = 40.2 \text{ mN m}^{-1}$) to predict encapsulation in waxy nanospheres (Lee et al., 1993), for ibuprofen in hydroxypropylmethylcellulose phthalate coacervates (Weiss, 1991) and for squalane in complex coacervates using various surfactants (Rabiskova et al., 1994). Finally, the importance of surface roughness and of shear forces for spreading of a polymer rich phase on a solid core material has also been addressed (Donbrow, 1992). These studies, along with our own results, have demonstrated that microencapsulation by coacervation is a dynamic and complex

process, for which interfacial properties can only be approximated. Nonetheless, the information gained from such measurements proves to be most useful for examining the very basic conditions for microencapsulation of a drug in a given system.

5.2. Entrapment and release of solid BSA

Besides interfacial and spreading characteristics, the surface area of the drug particles (solid or in solution) was shown to exert an important effect on the encapsulation efficiency. According to Eq. (7)

$$\Delta G = \Delta \gamma A \quad (7)$$

the surface free energy, ΔG , decreases if a drug particle moves from the equilibrium liquid ($\gamma_{P1/P3}$) into the coacervate phase ($\gamma_{P2/P3}$), due to a negative $\Delta \gamma$. In thermodynamic terms, the interaction energy solid BSA/coacervate is higher than that of solid BSA/equilibrium liquid. For given $\gamma_{P1/P3}$ and $\gamma_{P2/P3}$, ΔG is increased with higher surface area, A , of the core material. These considerations support our observations that most finely dispersed core material, as produced by ultrasonication of the protein solution or by the use of micronized powder, improved the encapsulation efficiency. However, for maintaining a natively high surface area during coacervation, coalescence of the aqueous protein droplets or aggregation of the solid particles must be prevented by vigorous agitation or adequate viscosity of the non-solvent, in agreement also with earlier reports (Donbrow, 1992). Furthermore, finely dispersed BSA was more uniformly entrapped, resulting in a lower burst release at moderate nominal loadings. By contrast, larger BSA particles were supposedly entrapped by deposition of a layer of coalescing coacervate droplets on the protein particles. This process, however, is counterbalanced by the non-solvent viscosity hindering an efficient polymer spreading on solid BSA. Similar findings were reported for cellulose acetate phthalate coacervates engulfing polystyrene beads of various sizes (Dittrich et al., 1993). However, the wall thickness of microspheres is not only determined by the particle size of the core material, but also by the nominal

loading and polymer concentration (Donbrow, 1986). In our study, increasing the core/wall ratios resulted in a higher burst, most probably due to a thinner polymer coat and matrix which could not separate the individual protein particles from each other. Consequently, a reservoir-like type of microspheres was produced (Fig. 3). When these low \bar{M}_w PLGA microspheres were incubated in the release medium, the thin polymer coat swoll and released a major part of the aggregated core material. Besides nominal loading and particle size of the core material, the polymer type, i.e. \bar{M}_w , copolymer composition, T_g and crystallinity, by virtue of swelling properties, also greatly affected the burst release, as shown here with semicrystalline PLLA.

In the literature, encapsulation efficiencies of 60–80% of solid drug material by coacervation were reported for histrelin (Lewis and Sherman, 1989), for triptorelin (Ruiz et al., 1989; Nerlich et al., 1993), for decapeptyl (Orsolini et al., 1986) and for tetanus toxoid (Thomasin et al., 1996a). In these studies, the amount released after 6 h varied between 6 and 57%, depending on the polymer characteristics and amount of PDMS used for coacervation. Encapsulation of 2–21 μm particle size BSA and of 15 μm particle size insulin into poly(L-lactide) and PLGA yielded efficiencies of 44–50% and 22–76%, respectively, depending on the type of hardening agent used (Komen and Groennendaal, 1991).

5.3. Entrapment and release of aqueous BSA

Both loading efficiency and burst release were highly sensitive to varying coacervation process parameters, and lower loading efficiencies were generally obtained with aqueous protein solutions as compared to micronized drug. Although the observed effects on loading efficiency and burst release must be multicausal, the viscosity of the coacervate and continuous phases is considered here as one of the principle parameters. Optimal viscosity of these phases was required to assure the stability of the coacervate droplets (against merging), to allow efficient spreading and coating of the coacervate phase on the dispersed BSA droplets and to act as a barrier against merging of

the engulfed BSA droplets. The following examples should illustrate the importance of a finely balanced viscosity.

Increasing amounts of PDMS decreased markedly the burst release. More efficacious drug entrapment was reported for higher coacervating agent/solvent ratios also for poly(ϵ -caprolactone) and PLA/PLGA using different drugs (Ruiz et al., 1989; Aftabrouhad and Doelker, 1994). For hydrocortisone acetate encapsulated in a block-copolymer of tartaric acid and 1,10-octanediol by coacervation, release was also influenced considerably by the coacervating agent/solvent ratio (Shively and McNickle, 1991); the authors related this finding not to viscosity effects, but to molecular surface area and configuration of the coacervated polymer, and to interaction properties, as determined by surface tension measurements.

With higher viscosity type PDMS, burst release increased, probably due to insufficient coating of the BSA droplets by the increasingly viscous system. This result is in agreement with the observation that encapsulation of riboflavin sodium phosphate was improved when PDMS of 1070 mPa s was replaced by PDMS of 110 mPa s (Aftabrouhad and Doelker, 1994).

Further viscosity influencing parameters were the polymer \bar{M}_w and initial polymer concentration. The low encapsulation efficiencies obtained at low polymer concentration can be ascribed, at least partly, to insufficient stabilisation of the emulsified aqueous BSA. Consequently, the size of the aqueous BSA droplets must have increased during coacervation. Concomitantly, due to the lower viscosity and volume of the coacervate phase at low polymer concentration, smaller size coacervate droplets (5–21 μm) were produced. These processes must have yielded an unfavourable size ratio of protein/coacervate droplets. Hence, a considerable fraction of protein must have not been well coated and removed by the washing procedure. At low polymer concentration, the loading efficiencies with the high \bar{M}_w (130 kDa) PLA microspheres did not differ from those obtained with the low \bar{M}_w (14.6 kDa) PLA, although the stability of the protein droplets was improved in the former system. We assume that the high molecular weight coacervate was too

viscous to spread efficiently on the aqueous protein droplets, resulting in a major fraction of unloaded coacervate droplets.

In conclusion, this study examined the impact of various interdependent process parameters in a given coacervation system. We have shown that PLA/PLGA coacervation represents a phase separation process characterised by continuous partitioning of polymer solvent and coacervating agent, thereby changing continuously the volume, the interfacial area and energy, and the viscosity of the coacervate. This is accompanied by changes in the interfacial shear stress and affinity between coacervate and solid or aqueous core material. This bears finally consequences for drug encapsulation and microsphere size. However, drug encapsulation remains difficult to predict as the interfacial properties change continuously with coacervate composition, which is basically a function of molecular interactions between polymer, solvent and coacervating agent.

Acknowledgements

We would like to thank Dr. E. Wehrli, Laboratory of Electron Microscopy I, ETH, Zürich, for providing the SEM micrographs, and Dr. U. Ohlerich, Krüss GmbH, Hamburg, for technical support in measuring interfacial properties.

References

- Absolom, D.R., Zingg, W. and Neumann, A.W., Interactions of proteins at solid-liquid interfaces: contact angle, adsorption, and sedimentation volume measurements. In Brush, J.L. and Horbett, T.A. (Eds.), *Proteins at Interfaces, Physicochemical and Biochemical Studies*, American Chemical Society, Washington, 1987, pp. 402–421.
- Aftabrouhad, S. and Doelker, E., Factors influencing the entrapment of a water soluble model drug into injectable microparticles using solvent evaporation and phase separation techniques. *Eur. J. Pharm. Biopharm.*, 40 (1994) 237–242.
- Bradford, M.M., A rapid and sensitive method for the quantitation of microgram quantities of protein utilizing the principle of protein-dye binding. *Anal. Biochem.*, 72 (1976) 248–254.

- Chang, T.M.S., Biodegradable semipermeable microcapsules containing enzymes, hormones, vaccines, and other biologicals. *J. Bioeng.*, 1 (1976) 25–32.
- Cohen, S., Yoshioka, T., Lucarelli, M., Hwaug, L.H. and Langer, R., Controlled delivery systems for proteins based on poly(lactic/glycolic acid) microspheres. *Pharm. Res.*, 8 (1991) 713–720.
- Dittrich, M., Melichar, L. and Smetanova, V., Influence of total surface area of core material on yield of deposited coacervate. *J. Microencapsulation*, 10 (1993) 45–54.
- Donbrow, M., Drug release kinetics and microencapsulation design. In Gorrod, J.W., Gibson, G.C. and Mitchard, M. (Eds.), *Development of Drugs and Modern Medicines*, Ellis Horwood, Chichester, 1986, p. 374.
- Donbrow, M., Developments in phase separation methods, aggregation control, and mechanisms of microencapsulation. In Donbrow, M. (Ed.), *Microcapsules and Nanoparticles in Medicine and Pharmacy*, CRC, Boca Raton, 1992, pp. 40–42.
- Dupre, A., *Théorie Mécanique de la Chaleur*, Paris, 1869, p. 368.
- Fong, J.W., Process for preparation of microspheres. *U.S. Patent*, 4,166,800, 1979.
- Fong, J.W., Microencapsulation by solvent evaporation and organic phase separation processes. In Hsieh, D. (Ed.), *Controlled Release Systems: Fabrication Technology*, Vol. 1, CRC, Boca Raton, 1988, pp. 81–105.
- Green, B.K., History and applications in microencapsulation. In Kondo, T. (Ed.), *Microencapsulation: New Techniques and Application*, Techno Books, Tokyo, 1979, pp. 1–9.
- Hora, M.S., Rana, R.K., Nunberg, J.H., Tice, T.R., Gilley, R.M. and Hudson, M.E., Release of human serum albumin from poly(lactide-co-glycolide) microspheres. *Pharm. Res.*, 7 (1990) 1190–1194.
- Kissel, T. and Demirdere, A., Microspheres — a controlled release system for parenteral application. In Müller, B.W. (Ed.), *Controlled Drug Delivery*, Wissenschaftl. Verlagsgesellschaft, Stuttgart, 1987, pp. 103–131.
- Komen, J. and Groennendaal, J.W., Process for microencapsulation. *U.S. Patent*, 5,066,436, 1991.
- Lapka, G.G., Mason, N. and Thies, C., Process for preparation of microcapsules. *U.S. Patent*, 4,622,244, 1986.
- Lawter, J.R. and Lanzilotti, M.G., Hardening agent for phase separation microencapsulation. *Eur. Patent Appl.*, 0 292 710 B1, 1992.
- Lee, H.K., Kwon, O., Park, J. and Kim, H., A novel quantitative criterion for the formation of nanoparticles. *Proc. Int. Symp. Control. Release Bioact. Mater.*, 20 (1993) 500–501.
- Lewis, D.H. and Sherman, J.D., Low residual solvent microspheres and microencapsulation process. *PCT Patent WO 89/03678*, 1989.
- Lu, W. and Park, T.G., Protein release from poly(lactic-co-glycolic acid) microspheres: protein stability problems. *PDA J. Pharm. Sci. Technol.*, 49 (1995) 13–19.
- McGee, J.P., Davis, S.S. and O'Hagan, D.T., The immunogenicity of a model protein entrapped in poly(lactide-co-glycolide) microparticles prepared by a novel phase separation technique. *J. Control. Release*, 31 (1994) 55–60.
- Nerlich, B., Gustafsson, J., Mank, R., Hörig, J. and Köchling, W., *Patentschrift DE*, 4223169 C1, 1993.
- Nihant, N., Grandfils, C., Jerome, R. and Teyssie, P., Microencapsulation by coacervation of poly(lactide-co-glycolide). IV. Effect of the processing parameters on coacervation and encapsulation. *J. Control. Release*, 35 (1995) 117–125.
- Orsolini, P., Mauvernay, R. and Deghenghi, R., Verfahren zur Mikrokapselung durch Phasentrennung von wasserlöslichen Arzneimittelsubstanzen. *Offenlegungsschrift DE* 3536902, 1986.
- Owens, D.K. and Wendt, R.C., Estimation of the surface free energy of polymers. *J. Appl. Polym. Sci.*, 13 (1969) 1741–1747.
- Rabiskova, M., Song, J., Opawale, F.O. and Burgess, D.J., The effect of interfacial hydrophobicity on the uptake of oil into complex coacervate microcapsules. In Süheyla Kas, H. and Atilla Hincal, A. (Eds.), *Minutes 9th Int. Symp. Microencapsulation*, Editions de Santé, Paris, 1994, pp. 76–79.
- Ruiz, J.M., Tissier, B. and Benoit, J.P., Microencapsulation of peptide: a study of the phase separation of poly(D,L-lactic acid-co-glycolic acid) copolymers 50/50 by silicone oil. *Int. J. Pharm.*, 49 (1989) 66–77.
- Ruiz, J.M., Busnel, J.P. and Benoit, J.P., Influence of average molecular weights of poly(D,L-lactic acid-co-glycolic acid) copolymers 50/50 on phase separation and in vitro drug release from microspheres. *Pharm. Res.*, 7 (1990) 928–934.
- Sanders, L.M., Kent, J.S., McRae, G.I., Vickery, B.H., Tice, T.R. and Lewis, D.H., Controlled release of a luteinizing hormone-releasing hormone analogue from poly(D,L-lactide-co-glycolide) microspheres. *J. Pharm. Sci.*, 73 (1984) 1294–1297.
- Sanders, L.M., Vitale, K.M., McRae, G.I. and Mishky, P.B., Controlled delivery of an LHRH analogue from biodegradable injectable microspheres. *J. Control. Release*, 2 (1985) 187–195.
- Sandow, J.K. and Seidel, H.R., Mikrokapseln von regulatorischen Peptiden mit kontrollierter Freisetzung, Verfahren zur ihrer Herstellung und Injektionszubereitungen. *Eur. Patent Appl.*, 0172422 A2, 1986.
- Shively, M.L. and McNickle, T.M., The physico-chemical effect of coacervation conditions on the diffusional properties and surface morphology of biodegradable microcapsules. *Drug Dev. Ind. Pharm.*, 17 (1991) 843–864.
- Thomasin, C., Corradin, G., Men, Y., Merkle, H.P. and Gander, B., Tetanus toxoid and synthetic malaria antigen containing PLA/PLGA-microspheres: importance of polymer degradation and antigen release for immune response. *J. Control. Release*, 41 (1996a) 131–145.
- Thomasin, C., Johansen, P., Alder, R., Bemsel, R., Hottinger, G., Altorfer, H., Wright, A.D., Wehrli, E., Merkle, H.P. and Gander, B., A contribution to overcoming the problem of residual solvents in biodegradable microspheres prepared by coacervation. *Eur. J. Pharm. Biopharm.*, 42 (1996b) 16–24.
- Thomasin, C., Merkle, H.P. and Gander, B., Thermodynamics of PLA and PLGA coacervation for microsphere formation. II. Experimental study. *J. Pharm. Sci.* (1996c) (submitted).

- Weast, R.C., Lide, D.R., Astle, M.J. and Beyer, W.Z., *CRC Handbook of Chemistry and Physics*, 70th edn, 1989, CRC Press, Boca Raton, p. F34.
- Weiss, G., Mikroverkapselung von Ibuprofen mit magensaftresistenten Polymeren durch einfache Koazervation. PhD Thesis, University of Regensburg, Germany, 1991.
- Young, T., In Peacock, G. (Ed.), *Miscellaneous Works*, Vol. 1, J. Murray, London, 1855.
- Van Krevelen, D.W., *Properties of Polymers*, Elsevier, Amsterdam, 1990, pp. 287–320.
- Zuidema, H.H. and Waters, G., Ring method for the determination of interfacial tension. *Ind. Eng. Chem.*, 13 (1941) 312–313.